Thermochimica Acta, 36 (1980) 367—375

THERMAL BEHAVIOUR OF CORONA-PRECIPITATED IODINE OXIDES *

A. WIKJORD, P. TAYLOR, D. TORGERSON and L. HACHKOWSKI

Atomic Energy of Canada Ltd., Whiteshell Nuclear Research Establishment, Pinawa, Manitoba ROE 1LO (Canada)

(Received 25 July 1979)

ABSTRACT

Oxo-compounds of iodine were produced by passing iodomethane and air through a negative corona discharge. Precipitates were collected from both the central electrode (cathode) and the discharge tube wall (anode). Thermogravimetry, differential thermal analysis, and X-ray diffraction measurements suggest that the cathode deposit was an amorphous form of I_2O_4 and that the anode deposit was an amorphous form of I_4O_9. The thermal analysis results show how corona iodine abatement procedures can be improved.

INTRODUCTION

We have recently introduced a new approach to gas phase iodine abatement which uses a corona discharge to promote reactions between active oxygen species and iodine compounds [1,2]. Small amounts of air-borne radioactive iodine can exist in various chemical forms in nuclear facilities, and filtering systems must efficiently purify very dilute iodine/air mixtures. The corona technique has been shown to remove both inorganic and organic iodine compounds effectively, including iodobenzene [1] which is difficult to filter using conventional techniques. Iodine is removed from air in the form of iodine oxide precipitates and characterization of these precipitates is important for ultimate product disposal.

Iodine—oxygen chemistry is complex and only a few iodine oxides have been well characterized. Oxo-compounds of iodine in the (I), (III), (V) and (VII) formal oxidation states have been reported [3,4]. The lower oxidation state oxides, I_2O and I_2O_3, have not been isolated although salts of the IO^+ and IO^- ions are known. The best-characterized iodine oxide is I_2O_5 which has a crystal structure consisting of O_2IOIO_2 molecules with extensive interaction through long intermolecular I- - -O contacts [5]. The iodine (III) and iodine(V) mixed oxidation state oxides, I_2O_4 and I_4O_9, are known, but have not been completely characterized. The structure of I_2O_4 is unknown, but the most recent spectroscopic study [6] favours an essentially monomeric structure, $OIOIO_2$, with long I- - -O interactions similar to those in I_2O_5 [5]. Little is known about I_4O_9; the suggested structure is iodine tri-iodate [4] but a molecular adduct formulation, $I_2O_4 \cdot I_2O_5$, is also plausible. The higher oxides I_2O_6 [7] and I_2O_7 [8] have been reported; I_2O_6 is thought to have the

* Issued as AECL 6291.

ionic structure, $IO_2^+IO_4^-$. The hydrated iodine oxides HIO_3 [9,10], HI_3O_8 [11] and H_5IO_6 [12] all have well-characterized crystalline structures, and several hydrates of I_2O_7 in addition to H_5IO_6 have been reported [3,13].

Although the structure and thermal stability of iodine oxy-acids and their salts have been reviewed recently by Solymosi [14], there are few reports on thermal behaviour of iodine oxides. Differential thermal analysis (DTA) or thermogravimetric (TG) measurements have been reported for only two iodine oxides — I_2O_5 and I_2O_4 — both in crystalline form; these studies appeared subsequent to a 1963 review [4] of iodine oxide structure and chemistry. There are no reports on the thermal behaviour of amorphous iodine oxides.

The thermal behaviour of crystalline I_2O_4 has been reported by Daehlie and Kjekshus [15] and Selte and Kjekshus [16]. It decomposes endothermally in the temperature range 375—500 K according to eqn. (1).

$$5\ I_2O_4 \rightarrow 4\ I_2O_5 + I_2 \qquad (1)$$

Above 575 K, I_2O_5 decomposes endothermally to the elements [15—17]

$$2\ I_2O_5 \rightarrow 2\ I_2 + 5\ O_2 \qquad (2)$$

EXPERIMENTAL

Samples were prepared by passing air at atmospheric pressure and loaded with ~100 μg/g iodomethane through the corona discharge tube shown in

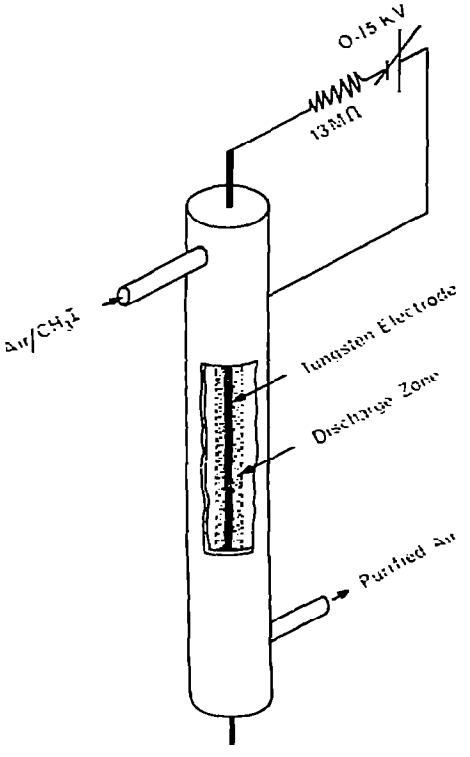

Fig. 1. Corona discharge tube used to produce iodine oxides.

Fig. 1. The central electrode was operated at ~ — 8000 V, and the resulting discharge removed greater than 99.99% of the iodomethane from the air stream. Details of the experimental procedures have been given previously [1].

Iodine compounds formed in the discharge tube precipitated on the walls and central electrode. On completing a run, the tube was transferred to a glove-box purged with dry nitrogen and deposits were removed from the walls and electrode.

Thermal behaviour of the iodine-containing deposits was studied by differential thermal analysis (DTA), thermogravimetry (TG) and X-ray diffraction. For the DTA and TG experiments, samples were heated at 20 K min^{-1} in platinum containers under an ~30 ml min^{-1} flow of argon (DTA) or nitrogen (TG). DTA curves were recorded on a DuPont 990 thermal analyzer coupled to a 1600°C furnace using a Pt vs. Pt—13% Rh thermocouple to measure the sample and reference temperature differences. Corundum (α-Al_2O_3) was used as the reference material for all DTA runs. TG curves were recorded with a Perkin—Elmer TGS-1 thermobalance. Sample temperatures were calibrated according to the Curie temperatures of magnetic standards [18]. X-ray diffraction measurements were made with a 114.6 mm Debye—Scherrer camera and a Guinier—Simon camera using Co$K\alpha$ and Cu$K\alpha_1$ radiations, respectively. DTA, TG and X-ray data were supplemented by mass spectrometry, X-ray fluorescence, and emission spectroscopy measurements.

RESULTS AND DISCUSSION

General

Uniform deposits were formed on the wall (anode) and filament (cathode) of the corona tube. These deposits were initially light yellow to light brown but became darker with time due to the release of free iodine. Iodomethane and elemental iodine both produced the same deposits, indicating that similar reaction mechanisms were involved. This suggests that the initial reaction with iodomethane probably involved cleavage of the C—I bond.

Fresh deposits from both the anode and cathode were amorphous, as determined by X-ray diffraction. However, heat, moisture, and aging were all observed to convert the precipitates to crystalline phases. Within 1—2 h following synthesis, samples changed colour and liberated elemental iodine even at room temperature. It was therefore necessary to characterize the deposits as soon as possible following synthesis, except where aging effects were being studied.

Direct probe mass spectroscopy and X-ray diffraction revealed similar thermal decomposition products for the anode and cathode products. On heating to 460 K, both products transformed to crystalline I_2O_5 with the liberation of I_2. On further heating above 600 K, the I_2O_5 decomposed completely into iodine and oxygen. Optical emission and X-ray fluorescence measurements showed that other elements, such as the electrode materials, were not present in the samples.

These general observations demonstrated that both products were iodine oxides with I : O atom ratios greater than 2 : 5. However, differences in thermal behaviour were observed and are discussed in the following sections.

Anode product thermal behaviour

DTA and TG data for the anode product are summarized in Fig. 2. The DTA curve for the fresh deposit (curve A) shows a small exothermic deflection at 415 K, a narrow exothermic peak at 460 K and a broader endotherm with a shoulder beginning at 630 K. The corresponding TG curve indicates that the exothermic reactions result in an 8% weight loss, and X-ray diffraction analysis shows that the product is crystalline I_2O_5. The exothermic transitions released elemental iodine which condensed on adjacent cool surfaces

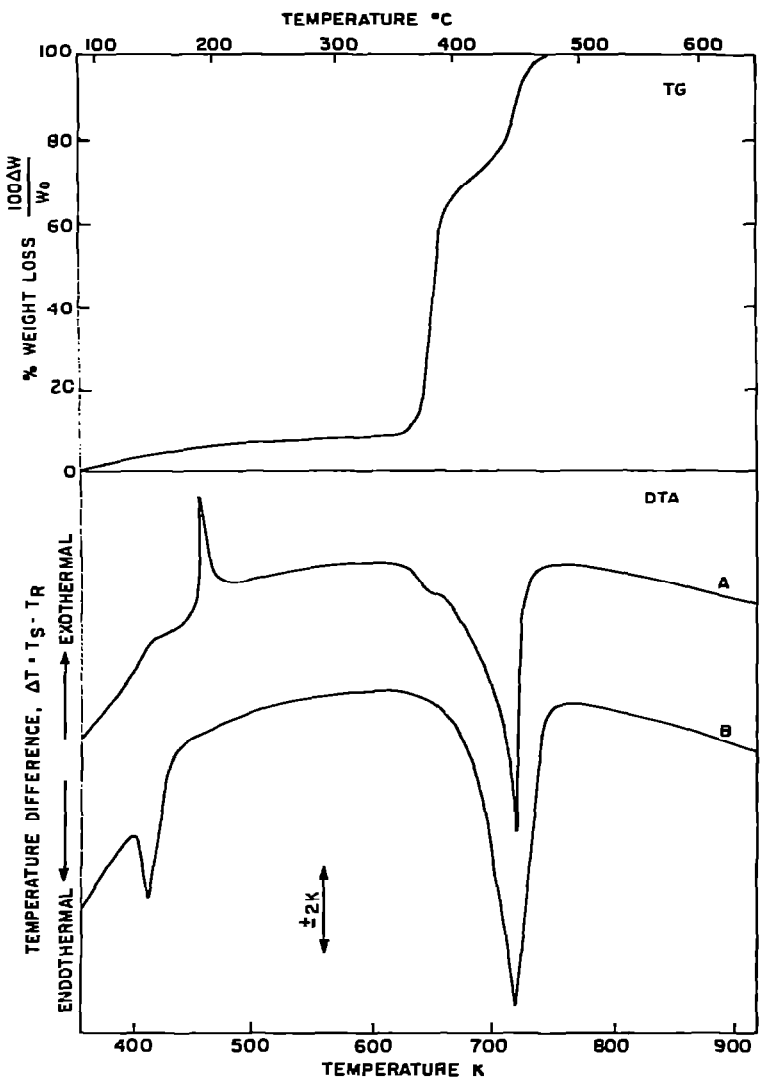

Fig. 2. Thermogravimetric and differential thermal analysis curves for the wall (anode) precipitate. Curves A and B are for fresh and 40-day aged samples, respectively.

in the DTA and TG instruments. These results are consistent with the initial product having the empirical formula I_4O_9 and decomposing according to

$$5\ I_4O_9 \rightarrow 9\ I_2O_5 + I_2 \qquad (3)$$

The theoretical weight loss for this reaction is 7.8%.

The high temperature endotherm results from the dissociation of I_2O_5 into its constituent elements. Both DTA and TG profiles reveal some fine structure in this region. The low temperature shoulder corresponds to a ~60% weight loss relative to the initial sample. This is hard to rationalize on a chemical basis and it is probably a physical effect, perhaps related to particle size. The effect was observed consistently with several anode deposits and similar behaviour for I_2O_5 has been reported previously [15]. The shoulder was absent or much less pronounced in the decomposition of I_2O_5 arising from cathode deposits, aged anode deposits, and commercial samples of HI_3O_8.

Also shown in Fig. 2 is a DTA measurement for the same sample obtained 40 days after synthesis (curve B). During this period, samples were stored in a desiccator, but there were frequent exposures to room air for sampling purposes. There are distinct differences between the DTA curves for the fresh and aged samples. For the aged sample, the exothermic reaction peak at 460 K has disappeared and an endothermic peak at 415 K has appeared. X-ray diffraction studies on the aged sample revealed the presence of a crystalline phase with a diffraction pattern (Table 1) that did not correspond to the *d*-spacings of any known iodine oxide or oxy-acid. The endothermic peak at 415 K corresponds to the decomposition of this unknown phase to form I_2O_5, as revealed by the I_2O_5 decomposition endotherm at 710 K. On heating the sample above 415 K in a closed tube, diffraction measurements using a high temperature Guinier camera showed that the crystalline hydrate HI_3O_8 was formed. It is likely that the dehydration products, I_2O_5 and H_2O, of the unknown hydrate recombined in the closed system to form the known hy-

TABLE 1

X-ray diffraction pattern for the crystalline hydrate formed from "amorphous I_4O_9"

d(pm)	Intensity	*d*(pm)	Intensity	*d*(pm)	Intensity
419	m	224	vw	183.7	m
375	s	217	vw	180.3	m
359	vw	212	vw	173.7	w
346	m	205.5	m	172.0	m
281	s	201.5	m	167.2	m
268	m	198.0	m		
261	w	190.5	m	plus ~ 40 lines to *d* = 90.7 pm	
239	vw	188.2	m		
231	vw	184.7	m		

m = medium, s = strong, vw = very weak, w = weak.

drate HI_3O_8

$$3\ I_2O_5 + H_2O \rightarrow 2\ HI_3O_8 \qquad (4)$$

Cathode product thermal behaviour

Thermal behaviour of the cathode deposit is different from the anode deposit as shown in Fig. 3. The initial amorphous phase is converted to I_2O_5 via two exothermic reactions peaking at 410 and 460 K. Diffraction studies showed that I_2O_5 was the only crystalline phase present following the transitions. The 17% total weight loss in this region was about twice that observed

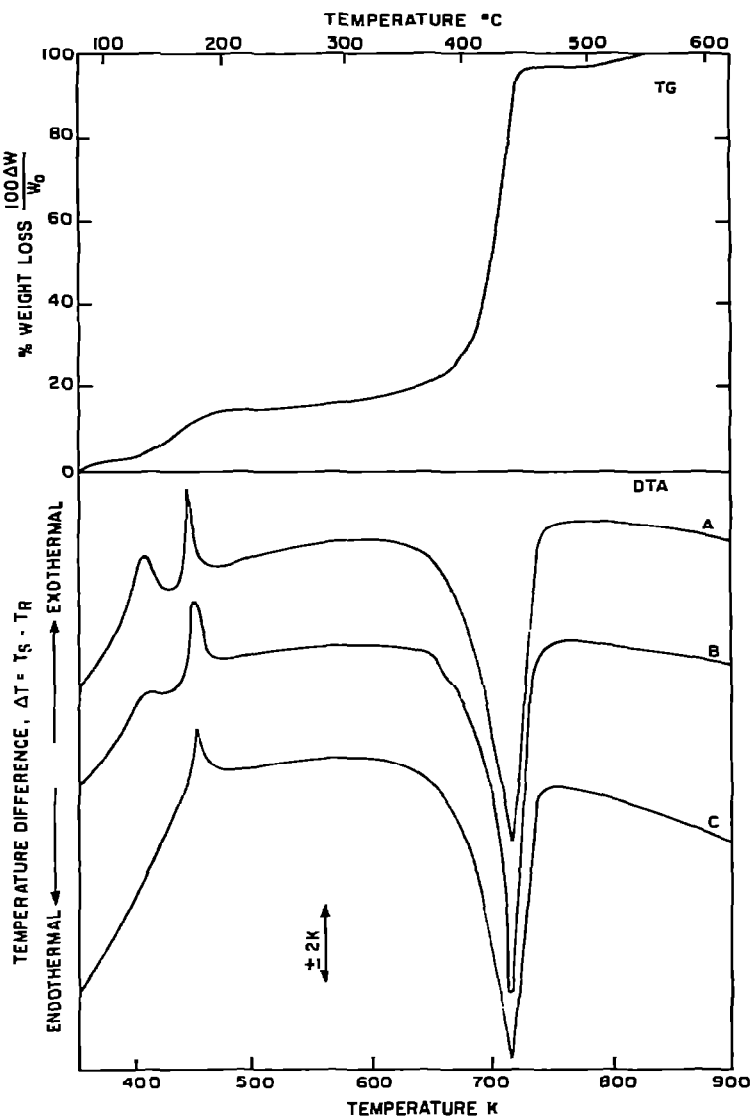

Fig. 3. Thermogravimetric and differential thermal analysis curves for the wire (cathode) precipitate. Curves A, B and C show how DTA characteristics vary with time. A = fresh sample, B = 8 days, C = 33 days.

for the anode material and is consistent with the following reaction

$5\ I_2O_4 \rightarrow 4\ I_2O_5 + I_2$ (16.0% theoretical loss)

The transformation of "amorphous I_2O_4" to I_2O_5 occurred by two exothermic steps peaking at 410 and 460 K, compared with the single endothermic reaction for crystalline I_2O_4 at 460—500 K reported by Daehlie and Kjekshus [15]. The lower transformation temperature and exothermic behaviour of our material are both consistent with the higher free energy of an amorphous material. Since the second exotherm at 460 K occurs at the same temperature as the exotherm observed for the anode product, I_4O_9, a likely reaction for the first step is

$$9\ I_2O_4 \rightarrow 4\ I_4O_9 + I_2 \qquad (5)$$

On aging, the 410 K exotherm gradually disappeared due to the slow conversion of amorphous I_2O_4 to I_4O_9 at room temperature, as shown in Fig. 3A, B and C. The 460 K exotherm also diminished somewhat, indicating partial decomposition of I_4O_9. There was no evidence for hydration of the I_4O_9 intermediate, perhaps owing to the fact that the original product I_2O_4 is not hygroscopic and exposure of the aged sample to moist air was minimal.

Precipitate formation

Information on precipitate formation mechanisms would require detailed knowledge of transient species present in the discharge tube. While these measurements are beyond the scope of the present work, some general observations can be made.

A negative corona discharge is maintained by positive ion bombardment of the central electrode, resulting in free electron emission. Near the wire, emitted electrons have sufficient energy to ionize the gas and produce more positive ions. This region is therefore characterized by a narrow discharge zone (3—4 mm diameter) in which relatively high energy processes are occurring. Iodomethane molecules in this zone may decompose and form positive ions due to electron impact. Iodine ions attracted to the wire would be subjected to a constant flux of positive ions such as O_2^+ and N_2^+. However, apparently only oxygen forms compounds with iodine under these conditions.

If the above mechanism dominates, it is difficult to explain why I_2O_4 is formed exclusively. Owing to the fact that there are $\sim 5 \times 10^4$ air molecules for every CH_3I, it is reasonable to assume that air accounts for most of the ionization. Gas phase reactions of the type

$$CH_3I + O_2^+ \rightarrow CH_3 + IO_2^+ \qquad (6)$$

could contribute significantly to iodomethane decomposition since it is known that decomposition rate depends on the oxygen concentration [1]. Moreover, the IO_2^+ ion has been observed in mass spectrometry studies [19] and is presumably a stable ion. Cathode reduction would then account for I_2O_4 formation

$$2\ IO_2^+ + 2\ \bar{e} \rightarrow I_2O_4 \qquad (7)$$

However, owing to the discharge region's complexity, it is possible that more complicated reactions are occurring.

Away from the central cathode the situation is quite different. Electrons no longer have sufficient energy to produce positive ions and electron capture processes dominate

$$O_2 + \bar{e} \rightarrow O_2^- \quad (8)$$

$$CH_3I + \bar{e} \rightarrow CH_3 + I^- \quad (9)$$

$$O_2 + \bar{e} \rightarrow O^- + O \quad (10)$$

Nitrogen does not form negative ions under corona discharge conditions [20]. The products of electron capture processes migrate towards the anode with nearly thermal velocities owing to the weak field outside the discharge region and high gas density. Only exothermic reactions with CH_3I are possible

$$CH_3I + O_2^- \rightarrow CH_3 + I^- + O_2 \quad (11)$$

$$CH_3I + O^- \rightarrow CH_3 + IO^- \quad (12)$$

Therefore, a variety of negatively charged species (e.g. I^-, IO^-, O_3^-) could be involved in the anode reactions and this is perhaps the reason for formation of I_4O_9 as opposed to a simpler compound such as I_2O_4 or I_2O_5.

The formation of these amorphous products by low temperature electrodeposition from the gas phase bears some similarity to other gas phase deposition processes whereby a wide variety of materials have been synthesized in amorphous states [21].

Iodine abatement

The thermal analysis results suggest that "corona iodine scrubbers" should be operated above ambient temperatures to promote formation of a stable precipitate (I_2O_5). This will prevent iodine leakage from the corona tube and will simplify precipitate handling procedures. Preliminary measurements have shown that abatement efficiencies increase with discharge tube temperature which may be related to I_2O_5 formation as well as the gas phase reaction kinetics.

ACKNOWLEDGEMENTS

We thank Mr. I Smith for collecting the samples used in this study and the WNRE support staff for their contributions to the gas scrubbing program.

REFERENCES

1 D.F. Torgerson and I.M. Smith, Proc. 15th DOE Nucl. Air Cleaning Conf., Boston, August 1978, Vol. 1, 1979, p. 437.
2 D.F. Torgerson and I.M. Smith, Atomic Energy of Canada Limited Report, AECL-5979 (1978).

3 A.J. Downs and C.J. Adams, in J.C. Bailar, Jr., H.J. Emeléus, R. Nyholm and A.F. Trotman-Dickenson (Eds.), Comprehensive Inorganic Chemistry, Vol. 2, Pergamon Press, Oxford, 1973, Chap. 26.
4 M. Schmeisser and K. Brandle, Adv. Inorg. Chem. Radiochem., 5 (1963) 41.
5 K. Selte and A. Kjekshus, Acta Chem. Scand., 24 (1970) 1912.
6 J.R. Dalziel, H.A. Carter and F. Aubke, Inorg. Chem., 15 (1976) 1247.
7 H. Siebert, M. Weise and U. Woerner, Z. Anorg. Allg. Chem., 432 (1977) 136.
8 H.C. Misra and M.C.R. Symons, J. Chem. Soc., (1962) 1194.
9 M.T. Rogers and L. Helmholz, J. Am. Chem. Soc., 63 (1941) 278.
10 R.S. Garrett, Oak Ridge National Laboratory Report, ORNL-1745 (1954).
11 Y.D. Feikema and A. Vos, Acta Crystallogr., 20 (1966) 769.
12 Y.D. Feikema, Acta Crystallogr., 20 (1966) 765.
13 H. Siebert, Fortschr. Chem. Forsch., 8 (1967) 470.
14 F. Solymosi, Structure and Stability of Salts in Halogen Oxyacids in the Solid Phase, Wiley-Interscience, New York, 1977.
15 G. Daehlie and A. Kjekshus, Acta Chem. Scand., 18 (1964) 144.
16 K. Selte and A. Kjekshus, Acta Chem. Scand., 22 (1968) 3309.
17 K. Jaky and F. Solymosi, Proc. Fourth Int. Conf. Therm. Anal., Budapest, 1974, Vol. 1, Heyden and Son, London, 1975, p. 433.
18 S.D. Norem, M.J. O'Neill and A.P. Gray, Thermochim. Acta, 1 (1970) 29.
19 M.H. Studier and J.L. Huston, J. Phys. Chem., 71 (1967) 457.
20 E.W. McDaniel, Collision Phenomena in Ionized Gases, Wiley and Sons, New York, 1964, pp. 373, 381.
21 D. Turnbull, Contemp. Phys., 10 (1979) 473.